MedCrave
Step into the World of Research

Journal of Stem Cell Research & Therapeutics

Research Article

Open Access

CrossMark

Therapeutic role of mesenchymal stem cells seeded dermal matrix versus acellular dermal matrix in healing of skin defect

Abstract

Background & objectives: One of the major challenges facing the surgeons is replacing a full-thickness skin loss successfully. This study aimed at testing the efficacy of decellularized dermal matrix seeded with bone marrow-mesenchymal stem cells (BM-MSCs) as a scaffold for the repair of skin defects in rats comparison to using acellular dermal matrix (ADM) alone.

Methods: A 2×2 cm^2 size full thickness skin defect was created on the dorsum of thirty male Wister rats (200- 250g) under xylazine (5 mg/kg) and ketamine (50 mg/kg) anesthesia. The animals were then randomly divided into three equal groups: *group I*; The defect was left for spontaneous recovery, *group II*; The defect was repaired with ADM alone, and *group III*;Tthe defect was repaired with ADM seeded with labeled BM-MSCs. The healing rate of the defect in all groups was assessed by measuring wound area and healing percentage twice weekly. The specimens from the wound site were obtained from all groups on day 14 and day 28 post-operative for histological analysis.

Results: Treatment of wound defect with BM-MSCs seeded dermal matrix resulted incomplete wound recovery on gross examination. Moreover, histological analysis showed proper reepithelization, proper collagen rearrangement together with minimal inflammatory cells. Well developed hair follicles and sebaceous glands were noted as well. Statistically, 28 days post-operatively, significant increase in healing rate, healing area percentage and collagen area percentage was detected together with significant decrease in vascular density compared to *group I&II*.

Conclusion: Stem cells seeded ADM facilitated early and better healing of skin defect in rats than the non- seeded ADM and spontaneous healing.

Keywords: acellular dermal matrix (ADM), bone marrow mesenchymal stem cells (BM-MSCs), bio-scaffold, skin defect

Volume 5 Issue 1 - 2019

Ghada F Mohamed, Manal H Moussa, Sahar MM Omar, Asmaa A Abo Zeid, Walaa Baher, Assem Mohammed, Mohamed Sobhy, Ahmed Sabry, Omar Adel, Mahmoud Salem, Omar Ahmed

Department of Histology, Armed Forces College of Medicine, Egypt

Correspondence: Sahar MM Omar, Histology Department, Armed Forces College of Medicine, Cairo, Egypt, Tel 00201001428289, Email saharhistology@gmail.com

Received: December 22, 2018 | **Published:** February 25, 2019

Introduction

Skin losses can occur due to acute trauma, resection of cutaneous malignancies, chronic wounds or even surgical interventions. The full thickness injuries are characterized by complete destruction of epithelial regenerative capacity which leads to extensive scarring.[1] The large wounds that cannot be corrected by conventional surgical procedures requires substitutes of missing tissue to keep the wound free of infection, reduce pain and ensure early wound healing.[2]

In autologous skin grafting donor site heal with some scarring and may be very painful. So, the need for tissue engineered construct became mandatory in which culturing the required cell types on a biocompatible scaffold or extracellular matrix (ECM) is performed.[3]

The scaffolds include synthetic biodegradable polymers, natural polymers and natural matrices derived from decellularized tissues. The natural bio-scaffold have advantages over synthetic material as it mimics natural ECM structure and composition, preserves natural stimulatory effects of ECM on cells and allows the incorporation of growth factors and other matrix proteins to further enhance cell functions.[4]

These natural matrices substitutes must exhibit three important properties; very low antigenicity, the capacity for rapid vascularization, and stability as a dermal template.[5]

Mesenchymal stem cells (MSCs) are characterized by the ability to self-renew and differentiate into multiple tissue-forming cell lineages. They have also been shown to exhibit immunomodulatory, reparative, and regenerative effects. Their ability to enhance cutaneous wound healing has been well characterized suggesting great therapeutic potential.[6] In this study, we aimed at comparing the usage of dermal matrix whether seeded with BM-MSCs or not in treatment of skin defects in rats compared to spontaneous healing. Our hypothesis was that applying BM-MSCs seeded dermal matrix to full thickness skin defect, would enhance and accelerate skin healing, and would restore the microstructure of the skin in comparison to unseeded ADM and spontaneous healing.

Materials and methods

All the animal procedures were approved by Faculty of Medicine-Ain Shams University Ethical Committee, and the experiments were conducted in accordance with their guidelines.

Preparation of acellular dermal matrix (ADM)[5]:

The skin of the back of seven male Wister rats (150-200g) was shaved, sterilized with betadine and 70% ethanol then dissected. Skin specimens were cut into pieces each 2×2 cm^2 and washed extensively with phosphate buffered saline (PBS). Then, washed in Roswell Park Memorial Institute (RPMI) 1640 Medium (Thermo Fisher Scientific, Cat. No: 11875093) containing 10% fetal bovine serum and preserved for further use at-20°C. For subsequent usage, the cryo

preserved skin is thawed at 37°C in PBS. For de-epithelization, the skin specimens were treated with buffered 1M NaCl for 24hours at 37°C with continuous shaking in an orbital shaker followed by simple scratching of the epidermis. Decellularization of dermal matrix was done by incubation in buffered 0.5% sodium dodecyl sulfate (SDS; Sigma Chemical Co., St. Louis, MO) for 1hour at room temperature in an orbital shaker. Acellular dermal matrix treated with NaCl-SDS was then extensively washed with PBS and stored in PBS at 4°C until usage. All solutions used for ADM preparation were filtered with 0.2µm filter. Antibacterial (300U/ml penicillin, 0.3mg/ml streptomycin) and antifungal (0.75µg/ml amphotericin B) were added to the extraction solutions to prevent microbial growth.

Isolation, culture and labeling of BM-MSCs7:

In brief, both ends of tibias and femurs of rats were cut from the diaphysis. The bone marrow was flushed out from the bone with Dulbecco's Modified Eagle's medium (DMEM, Life Technologies) containing 10% FBS, 1% penicillin/ streptomycin. The marrow plugs were then dissociated by pipetting and centrifuged at 1800 rpm for 10min at 4°C. The precipitated cell pellets were re suspended with 5 ml of the complete medium. The cells were then seeded into 25 cm^2 tissue culture flasks at a density of 7×10^5 cells/cm^2 and kept at 37°C in a humidified incubator containing 5% CO_2. The culture medium was replaced every 3 days.

The second passage cells were labeled by PKH26 Red Fluorescent Cell Linker Kit for General Cell Membrane Labeling (Molecular probes, Sigma-Aldrich, St. Louis, Mo, USA) according to the manufacturer's instructions. Briefly, the cells were mixed with PKH26 reagent and incubated at 25°C for 2-5min with gentle shaking. The staining action was blocked by adding an equal volume of serum and incubated for 1min. Then, the cells were centrifuged at 1800rpm for 10min at 25°C. The supernatant was removed; the cells were transferred into a new tube and washed three times with PBS. Finally, 10 ml of complete culture medium was added to the cells to be centrifuged and adjusted to a density of 1×10^6 cells/ml.[8]

Seeding of labeled MSCs on ADM

The ADM was used as scaffold for the culture of BM-MSCs using the static seeding technique.[9] The ADM was placed on 35 mm Petri dishes, the labeled MSCs were seeded on the reticular surface of ADM at a concentration of 5×10^5 cells/cm^2 and incubated for 48hours. The cell-laden ADM was washed several times with PBS to remove remnants of culture media, then transplanted and sutured to the edges of the skin defect.

Histological analysis of ADM

Specimens of ADM were processed for histological examination. They were fixed with 10% phosphate-buffered formalin, dehydrated and processed to obtain paraffin blocks. Sections (5µm) were stained with H&E stain and Masson's trichrome stain. Other specimens were fixed in 2.5% glutaraldehyde for transmission electron microscopy. Samples were dehydrated by an ascending series of alcohols and then embedded in epoxy resin. Sections (60-80 nm) were cut by an ultra microtome, stained with lead citrate and uranyl acetate, examined and photographed with Jeol, JEM- 1200 EX II Electron Microscope, Tokyo.

Animal groups:

Thirty male Wister male rats with weights between 200 and 250 g were used in this study. The skin of the dorsum of all rats was shaved, sterilized with betadine and 70% ethanoland a $2\times2cm^2$ size full thickness skin defect was created under xylazine (5mg/kg) and ketamine (50mg/kg)anesthesia.

The animals were kept under standard housing conditions and provided with water and standard diet ad libitum.

After creating the wound, the animals were randomly divided into three equal groups (n=10):

1. **Group I:** The defect was left for spontaneous healing
2. **Group II:** The defect was repaired with unseeded ADM
3. **Group III:** The defect was repaired with labeled BM-MSCs-seeded dermal matrix

The grafts in groups II and III were sutured carefully by synthetic absorbable suture material (polyglycolic acid) and bandaged well with Vaseline gauze. All animals received topical and systemic antibiotics, as well as analgesics for three days postoperative. In each group, half of the animals (n=5) were sacrificed post-operative on day 14, and the remaining half (n=5) were sacrificed on day 28 post-operative.

Wound examination:

1. Gross observation:

Skin wounds were observed grossly and photographed in all groups post operatively on day 14 and day 28.

2. Histological examination:

The specimens from the wound sites were obtained from all groups on day 14 and day 28 post-operative for the histopathological examination after sacrificing the animals. Tissue samples were collected by excising the graft with a surrounding rim of normal skin and fixed in phosphate buffered10% formalin saline, dehydrated in ethanol, cleared in xylene and embedded in paraffin to get 5-micron thick paraffin sections. The sections were stained with H&E stain for detection of signs of wound healing and Masson's Trichrome stain to observe the collagen fiber density, thickness and their arrangement at the graft site. Paraffin unstained sections from the grafts of group III were examined under the fluorescence microscope for detection and tracing the PKH26-labelled MSCs.

3. Morph metric and Statistical analysis:

The following parameters were measured:

a. **Percent change in wound area:** To measure wound area, the length and width of the wound were identified as the largest diameter of the wound and diameter taken at right angle to the largest one. Measurements were done with a conventional metric ruler and expressed as area recorded in square centimeters (cm^2).

To calculate percent area reduction from baseline at the end of the experiment (day 28), the following formula was used: %Reduction = 100 x (baseline - current size)/baseline0[10]

Rate of wound healing: The rate of wound healing was defined as the change in wound area over 2 weeks using the following formula:

$$\Delta A_{(a-b)} = \left(A_b - A_a\right) / \left(b - a\right)$$

Where (A) equals area, (a) equals the beginning of the observation period, and (b) equals the end of the observation period.[11]

b. **Density of vascular structures (number of capillaries/ field):**

c. **The mean of area percentage of collagen:** Five specimens from five different rats of each group on day 14 and day 28 were examined (n=5). For each specimen, five different non-overlapping fields were analyzed using Leica Qwin V3 computer□assisted image analysis software (Leica Microsystem, Wetzlar, Germany). Numerical values obtained from mathematical calculations and morph metric measurements were expressed in means±standard deviation (SD) and analyzed using SPSS software (IBM Inc., Chicago, Illinos, USA). In which one-way analysis of variance (ANOVA) was performed, followed by post hoc least significance difference (LSD) for comparison between groups. P value≤0.05 was considered statistically significant.

Results

Morphological characteristics of ADM

Morphological characterization of ADM was done in comparison to normal skin specimens using light and electron microscopy.

Normal skin

Sections stained with **H&E**, showed that skin was formed of two layers; superficial *epidermis*, composed of stratified squamous keratinized epithelium and underlying *dermis*, composed of dense, irregular connective tissue that is divided into a superficial papillary layer and a deeper more extensive reticular layer with no distinct boundary between them. (Figure 1)

The dermal papillary layer appeared composed of thin, loosely arranged fibers and cells together with capillary loops, whereas, the dermal reticular layer which constitutes the major portion of the dermis has dense bundles of collagen fibers. Skin appendages as hair follicles, sebaceous and sweat glands were clearly demonstrated in the dermis (Figure 1a & 1b).

Masson's trichrome: stained sections showed the different arrangements of collagen in the dermis into loose fibers in the papillary layer and dense collagen bundles in the reticular layer (Figure 1c).

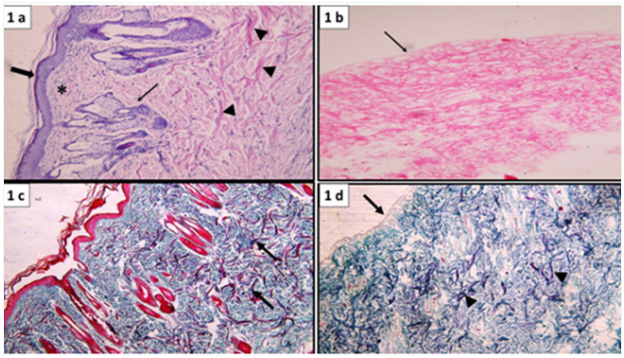

Figure 1 (a) Normal skin showing intact epidermal layer formed of stratified epithelium (thick arrow), lying over connective tissue dermis formed of superficial papillary layer containing loosely arranged fibers and cells (*) and deep reticular layer containing collagen bundles (▲) hair follicles and associated sebaceous glands (↑). **(b)** Acellular dermal matrix (ADM) showing absence of epidermal cells (arrow), the underlying dermis shows acidophilic collagen fibers and absence of basophilic nuclei. (a&b: H&E, x100). **(c)** Normal skin showing dense collagen bundles in the deep dermal layer (arrow). **(d)** ADM showing intact basement membrane (arrow) and dense collagen bundles in the deep dermis (▲) (c&d: Masson's trichrome stain, x100).

Ultra structural: Examination showed epidermal cell layers separated from the underlying dermis by basement membrane. (Figure 2) The dermis appeared formed of collagen bundles and fibroblasts (Figure 2a).

Acellular dermal matrix: H&E: Staining of skin specimens treated with hypertonic solution (NaCl) and ionic biological detergent (0.5% SDS) to obtain ADM confirmed complete removal of the epidermal cell layers (de-epithelization).Moreover, Decellularization of the dermis was indicated by absence of dermal connective tissue cells, blood vessels and skin appendages (Figure 1b).

Masson's trichrome: Stained sections demonstrated intact basement membrane. Collagen fibers' arrangement remained unaltered as compared to that of normal skin (Figure 1d)

Ultra structural: Examination revealed that, all keratinocytes were removed while the integrity of the basement membrane was maintained. There was no evidence of cells within the dermal matrix. The collagen bundles of the dermis showed similar arrangement and compactness as control (Figure 2b).

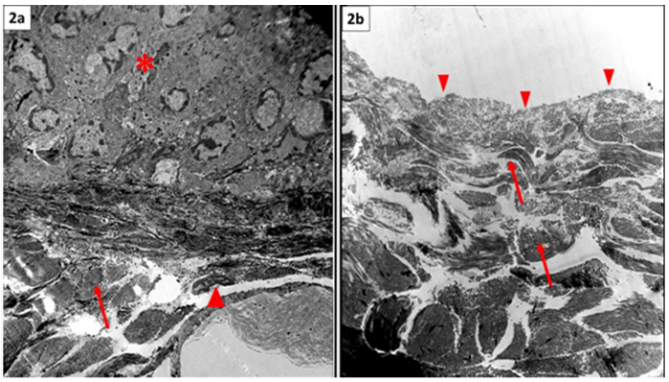

Figure 2 (a) Normal skin showing stratified epidermis (*) resting on basement membrane, the underlying dermis shows collagen bundles (arrow) enclosing in between connective tissue cells (▲). (b) ADM showing absence of the epidermal layer, intact basement membrane (▲) and preserved collagen bundles of the underlying dermis (arrow). Note absence of nuclei in between fibers (TEM, x3000).

BM-MSCs examination: Using *phase contrast microscope*, MSCs isolated from rat bone marrow showed fibroblast-like cells interconnected with each other through their processes forming colonies in primary culture (Figure 3a). Tracing seeded PKH26 labeled MSCs onto the ADM using *fluorescent microscope*, revealed red fluorescence with an excitation wavelength of 565nm, indicating incorporation of MSCs into ADM (Figure 3b). Furthermore, dermal grafts obtained from wound sites after 28 days of the operation from group III, revealed red fluorescence signals from PKH26-labelled BM-MSCs, indicating the well distribution and survival of MSCs seeded on the ADM (Figure 3c).

Gross observation of the wound

On gross observation, group Ion (Day 0) (day of wound creation), the wound was expanded initially as no graft was used in this group and the site of wound remained denuded (Figure 4). In groups II and III, the wound defects were covered with ADM graft (whether seeded or not), both appeared whitish in color (Figure 4a–Figure 4c).

On day (D14): Group I, the site of wound appeared slightly bulged, dried and covered with dark brown thick crust (Figure 4d). In group II, the graft appeared brown red and the wound edge looked

smooth compared to group I (Figure 4e). In group III, the wound was markedly reduced in size and nearly healed (Figure 4f).

On day (D28): The crust has fallen off and wound appeared covered with scar. Neither decrease in the size of the wound nor hair growth was evident in group I (Figure 4g). In group II, the wound was greatly shrunken in size with no scar formation (Figure 4h). In group III, there was no visible wound and wound site appeared completely healed and covered with hairy skin (Figure 4i).

Histological examination of the wound postoperative

H&E staining

On day (D14): Microscopic examination of skin sections stained with H&E showed:

Group I: The defect was filled with granulation tissue that showed severe inflammatory reaction. (Figure 5) Furthermore, the superficial layer of the granulation tissue showed sloughing, necrosis together with extravagated RBCs and abundant inflammatory cells (Figure 5a).

Group II: The superficial surface of the dermal graft was covered completely with a thin layer of epithelium. Revascularization of the matrix stroma was evidenced by the presence of numerous blood vessels. Furthermore, the acellular dermal matrix exhibited recellularization with mild inflammatory infiltrate (Figure 5b).

Group III: The wound site was re-epithelized by typical epidermal layer, the matrix was infiltrated by cells mostly fibroblast with minimal inflammation (Figure 5c).

On day (D28): Microscopic examination of skin sections stained with H&E showed:

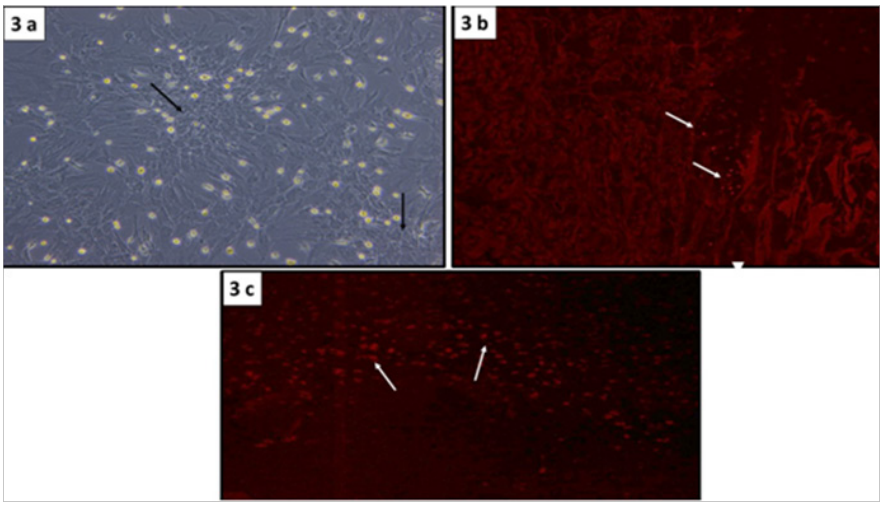

Figure 3 (a) Confluent monolayer of BM-MSCs with a fibroblast-like morphology forming colonies (↑) (Phase contrast microscopy, x100). **(b)** PKH26 fluorescent-labeled BM-MSCs seeded onto ADM (↑). **(c)** Distribution of PKH26-labeled BM-MSCs in the ADM, 28 days after transplantation (↑) (b&c: fluorescence microscopy, x100).

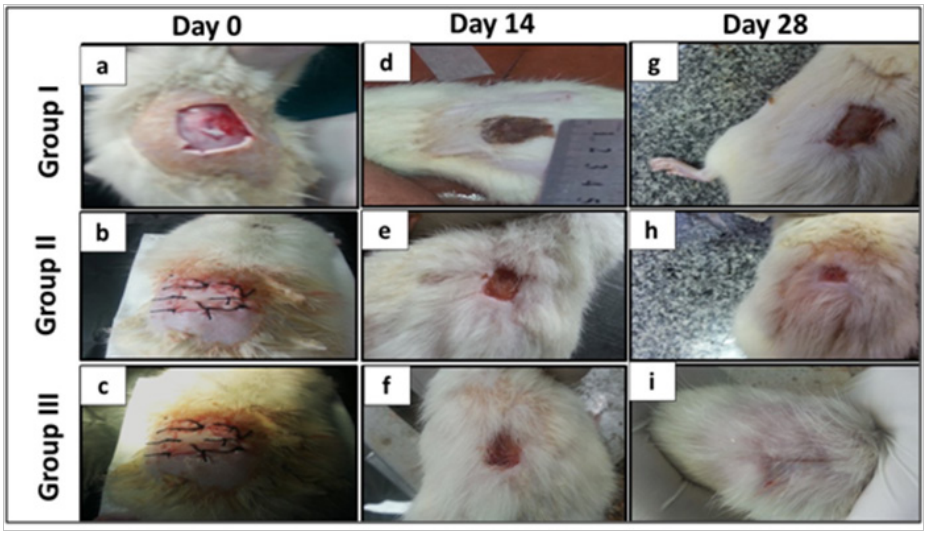

Figure 4 showing gross appearance of the wound on Day 0: (a) Group I: The wound defect (2x2cm) is left for spontaneous recovery, wound edges expand initially as no graft is used and the site of wound is denuded. (b, c) Groups II & III: The wound is covered with whitish ADM that is sutured to the wound edges. Day 14 (d) Group I: Wound edges are slightly bulging, and dark brown thick crust is covering the wound. (e) Group II: the graft is brownish red in color and the wound edges are smooth. (f) Group III: The wound surface is brownish pink in color with smooth edges. Note the remarkable decease in wound size. Day 28: (g) Group I: The crust is fallen off and the wound is covered with scars. Note that there is only slight decrease in the wound size. (h) Group II: The wound is remarkably decreased in size with no scar formation. (i) Group III: wound is almost invisible and wound site is covered with hairy skin.

Group I: A thick layer of granulation tissue appeared covering the wound defect. The granulation tissue is formed of layers of connective tissue cells embedded in acidophilic matrix and overlying heavy inflammatory reaction. (Figure 6) The dermis showed new blood vessels and thin disorganized collagen fibers (Figure 6a).

Group II: The dermal matrix was completely covered with typical stratified squamous keratinized epithelium of the epidermis. The graft matrix showed neovascularization, intact collagen bundles that became repopulated with fibroblasts. Inflammatory reactions were subsided as well (Figure 6b).

Group III: The healing was complete with typical epidermal layer. The dermis was repopulated with connective tissue cells, neovascularization was minimal and collagen fibers were best arranged comparable to normal skin. Inflammation was absent. Well-developed hair follicles and sebaceous glands were seen in the dermis (Figure 6c).

Masson's trichrome staining

On day (D14): Examination of Masson's trichrome stained section revealed (Figure 7):

Group I: The collagen fibers were minimal, less dense, and arranged haphazardly forming the granulation tissue filling the wound (Figure 7a).

Group II: The collagen fibers in the dermal matrix appeared thin, less dense and less regularly arranged (Figure 7b).

Group III: Areas of mature collagen bundles appeared at healing sites mainly in the reticular dermis (Figure 7c).

On day (D28): The following results were demonstrated:

Group I: The collagen fibers in the dermis became thicker with better arrangement (Figure 7d).

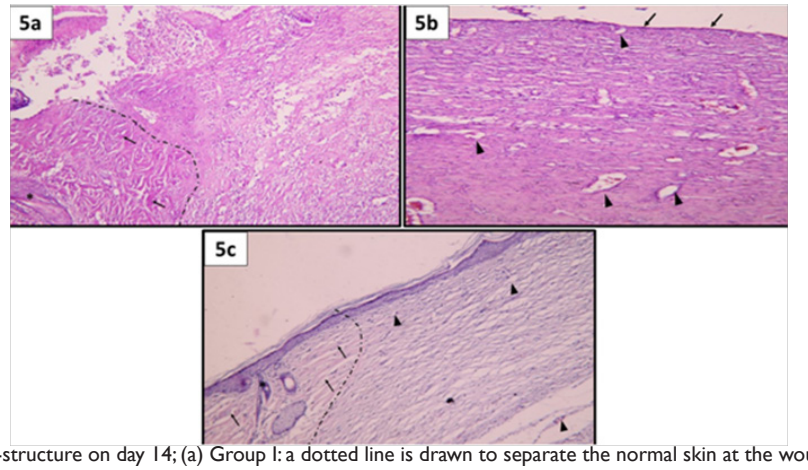

Figure 5 Showing wound micro-structure on day 14; (a) Group I: a dotted line is drawn to separate the normal skin at the wound edge (on the left side) from the wound site (on the right side). Notice the presence of well-formed collagen bundles (*) and the presence of hair follicles (↑) on the normal wound edge. On the other hand, the wound site is filled with sloughed granulation tissue that show necrosis together with extravagated RBCs and abundant inflammatory cells. No epidermis is seen. (b) Group II: The dermal graft surface is completely covered by a very thin layer of epidermis (↑). Evident revascularization of the matrix stroma (▲). Notice that, the ADM exhibited recellularization with mild inflammatory infiltrate. (c) Group III: A dotted line is drawn separating the normal skin edges (on the left side) from the wound site (on the right side). Notice the presence of thick collagen bundles (↑) as well as hair follicles and sebaceous glands (*) in the normal wound edge. On the right side, the wound site shows complete reepithelization,by typical epidermal layer, the matrix is infiltrated by cells mostly fibroblast with minimal inflammation. Notice the presence of blood capillaries in the dermal matrix (▲). (H&E, x100).

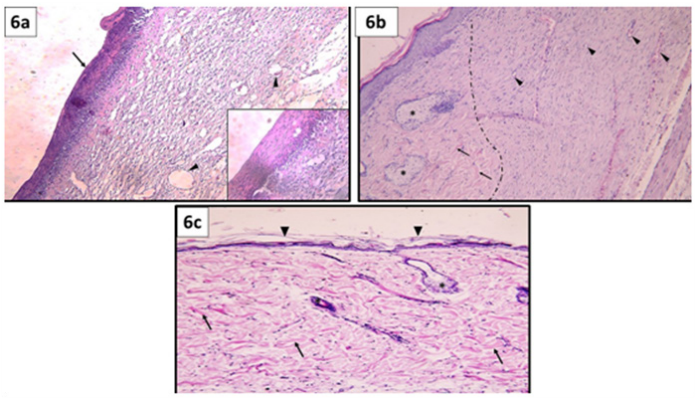

Figure 6 Showing wound micro-structure on day 28 (a) Group I: The wound is covered by a thick layer of granulation tissue (↑). The granulation tissue is formed of layers of connective tissue cells embedded in acidophilic matrix and overlying heavy inflammatory reaction (inset). The dermis is formed of disorganized thin collagen with marked neovascularization (▲). (b) Group II: a dotted line is drawn separating normal skin edges (on the left side) from the wound site (on the right side). Normal skin edges show well organized collagen bundles (↑) and well-formed sebaceous glands (*). On the other hand, the dermal matrix was completely covered with typical stratified squamous keratinized epithelium of the epidermis. The graft matrix shows intact collagen bundles that became repopulated with fibroblasts. Notice the presence of many blood capillaries (▲) and absence of inflammatory reaction. (c) Group III: The epidermis over the dermal matrix at the wound site shows complete reepithelization (▲). The dermis shows well organized thick collagen bundles (↑), connective tissue cells, hair follicle and sebaceous gland (*). Notice the absence of inflammatory reaction and minimal neovascularization in the dermis. (H&E, x100).

Citation: Mohamed GF, Moussa MH, Omar SMM, et al. Therapeutic role of mesenchymal stem cells seeded dermal matrix versus acellular dermal matrix in healing of skin defect. *J Stem Cell Res Ther.* 2019;5(1):13–21. DOI: 10.15406/jsrt.2019.05.00128

Group I: Collagen fibers were more organized into thin bundles (Figure7e).

Group III: Mature collagen bundles occupying the whole graft were comparable to that of normal skin (Figure 7f).

Statistical analysis results (Table 1):

Wound healing rate: Over the first 2 weeks showed a non-significant change in groups II and III. However, a significant increase between these groups in comparison to group I was identified. Over the second 2 weeks, group III showed the maximum rate of wound healing that was significant to both group II and group I. Similarly, group II recorded a significant increase in the healing rate in comparison to group I (Histogram 1).

Although, group I showed a remarkable increase in the wound healing rate over the second 2 weeks in comparison to the first 2 weeks, the *percentage of wound reduction area* at the end of the experiment, was only 66.4±3.61%. On the other hand, groups II and III, showed a higher significant wound reduction area percentage (92.8±1.58% and 99.6±0.46% respectively) in comparison to group I (Table 1).

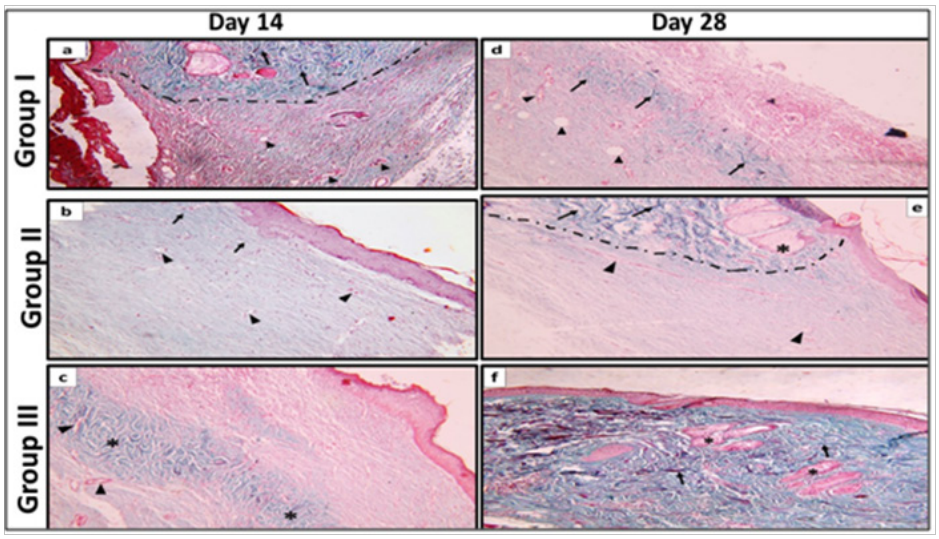

Figure 7 Showing dermis of the wound, on **Day 14 (a) Group I:** A dotted line was drawn to separate the normal wound edges from the wound site. Notice the presence of well-formed thick collagen bundles () on the normal wound edges. On the contrary, the wound site shows minimal amount of dispersed collagen fibers enclosing blood capillaries in between (▲). **(b) Group II:** The dermis is formed of thin dispersed collagen fibers with occasional thin bundles (↑) enclosing blood capillaries in between (▲). **(c) Group III:** Areas of thick collagen bundles are identified in the reticular dermis (*) with blood capillaries in between (▲). **On day 28 (d) Group I:** Areas of relatively thick collagen bundles (↑) and wide blood capillaries are seen in the reticular dermis (▲). **(e) Group II:** A dotted line was drawn separating normal skin edge from the wound site. Thick collagen bundles (↑), hair follicles and sebaceous glands (*) appear in dermis of normal skin edge. At the wound site, blood capillaries (▲) and less organized, thin collagen bundles appear dispersed in the dermis. **(f) Group III:** The dermis at the wound site contains well-organized, thick collagen bundles (↑) in both the papillary and reticular layers. Notice the presence of hair follicles and sebaceous glands (*). (Masson's richrome stain, x100).

Table 1 Values of Means±Standard deviation of different parameters in experimental groups

Groups	Group I	Group II	Group III
Wound healing rate over the first 2 weeks	0.12±0.084 (*●)	0.73±0.087 (▲)	0.84±0.063 (▲)
Wound healing rate over the last 2 weeks	0.62±0.013 (●)	0.82±0.016 (●)	1.1±0.012 (▲*)
% reduction in SA	66.4±3.61 (●*)	92.8±1.58 (● ▲)	99.6±0.46 (▲*)
Area percentage of collagen on Day 14	23.2±1.96 (*●)	37.32±3.45 (● ▲)	41.2±1.02 (▲*)
Area percentage of collagen on Day 28	33.1±2.67 (*●)	43.2 ±3.58 (● ▲)	53.1±6.9 (▲*)
Vascular density on Day 14	17.2±0.84 (*●)	24.6±1.14 (● ▲)	32.2±1.3 (▲*)
Vascular density on day 28	44 ±2.38 (*●)	26.2± 2.68 (● ▲)	20±1.58 (▲*)

(▲), Significant change from group I; (*), Significant change from group II and (●), Significant change from group III.

Area percentage of collagen fibers on days 14 and 28: Illustrated a significant increase in group III in comparison to group II and group I. Also, in group II, a significant increase was identified on days 14 and 28 in comparison to group I (Histogram 2).

Vascular density on day 14: Showed a significant increase in group III in comparison to group II and group I. In contrast, on day 28 group I showed a significant increase in the vascular density in comparison to group II and group III. Likewise, there was a significant increase in group II in comparison to group III on day 28 (Histogram 2).

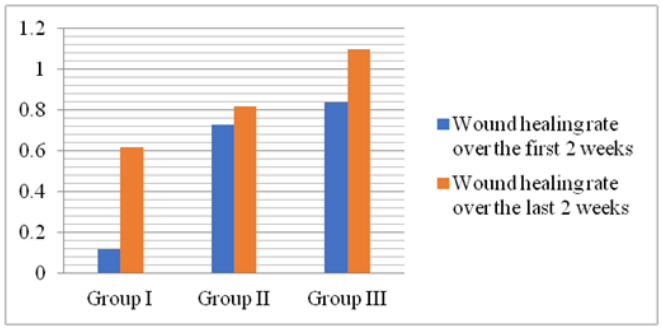

Histogram 1 Mean values of wound healing rates in different groups.

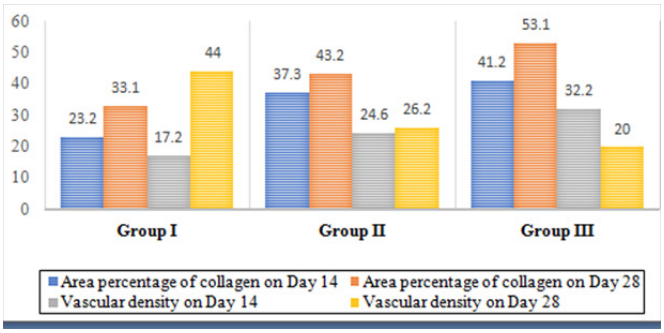

Histogram 2 Mean values of collagen area percentage and vascular density in different groups on days 14 and 28 postoperative.

Discussion

Wound healing is a complex process that requires the coordinated interplay of ECM growth factors and cells.[12] The need to replace skin lost through injury is particularly crucial in extensive wounds. Skin can be obtained from donors; however, the inevitable rejection of allogenic skin has limited its major use for wound coverage.[13]

However, immunological complications associated with skin grafting that contain allogenic cells, can be avoided by utilizing acellular matrix scaffolding into which patient's own cells can migrate.[13]

In current work, ADM was obtained using hypertonic NaCl that dissociates DNA from proteins followed by SDS detergent that solubilized cell membranes. Characterization of this matrix was done by light microscope using two different stains (H&E and Masson's Trichrome) and by electron microscope to ensure the resemblance of this matrix after treatment with NaCl-SDS to the matrix of untreated normal skin.

It is obvious that, cell removal agents and techniques alter ECM composition and cause some degree of ultra structure disruption. Hence, minimization of these undesirable effects rather than complete avoidance is the objective of Decellularization process.[12]

Walter et al.[5] compared NaCl-SDS and Dispase-Triton methods in the preparation of ADM. They reported that presence of larger amounts of type IV and VII collagen, laminin, fibronectin, desmin, and elastic in the NaCl- SDS ADM could support cell attachment and proliferation. Removal of cells and cellular components from dermis in ADM, leaves the natural mixture of structural and functional proteins that constitute the ECM, such as collagen, fibronectin, laminin and vimentin,[14] providing a natural microenvironment for cell adherence and expansion. Furthermore, endogenous growth factors such as fibroblast growth factor-2 (FGF-2) and transforming growth factor beta (TNF-β) often remain on naturally derived scaffolds which might facilitate cell growth on the ADM.[15]

Before proceeding to discuss the results of the present study in different groups, a brief summary of the normal process of wound healing should be noted. Normal wound healing is a dynamic and complex process involving a series of coordinated events that occur in three overlapping phases.

Inflammatory phase: In which neutrophils, monocytes and macrophages are attracted to the wound site to phagocytose damaged structures and secrete potent tissue growth factors.

Proliferative phase: In which reepithelization, fibroblast migration, deposition of newly synthesized ECM, an abundant formation of granulation tissue and angiogenesis occur. Fibroblasts attach to the fibrin matrix and begin to produce disorganized collagen.

Remodeling phase: In which the tensile strength of the wound increases progressively in parallel with collagen deposition that becomes more oriented and crosslinked over time.[16]

In the current study, wound healing was observed and examined postoperatively at two-time intervals on the 14th and the 28th days in all groups. In group I (spontaneous healing), inflammatory reaction was detected intensively on day 14 and was not resolved until day 28. In groups II (unseeded ADM) and III (MSCs seeded ADM), the inflammatory reaction was minimal on day 14 with complete resolution on day 28 especially noted in group III.

These results could be explained in the view of Feng et al.[17] who deduced that the application of ADM on wound may decrease the occurrence of sepsis which in turn prevent progressive wound infection and facilitate wound healing.

Furthermore, in group III, seeding MSCs onto ADM resulted in early resolution of inflammation due to the known anti-inflammatory and antimicrobial activity of MSCs. MSC antimicrobial activity is mediated both directly, via secretion of antimicrobial factors,[18] and indirectly, via secretion of immune- modulative factors, which will up regulate bacterial killing and phagocytosis by immune cells.[16]

In the present study, minimal reepithelization was observed on day 14 and was almost completed on day 28 in group II (unseeded ADM). In group III (MSCs seeded ADM), complete reepithelization with complete epidermal layer covered with keratin was seen on day 14, which became more mature on day 28. However, no reepithelization was detected what so ever in group I (spontaneous healing).

Two independent and complementary mechanisms could explain wound re-epithelialization. A sliding mechanism; in which passive lateral displacement of the superficial layers near the wound margin toward the free space over the wound due to the pushing force from the proliferating basal keratinocytes of the adjacent unwounded epidermis. This displacement is favored by the absence of resistance from the wound side due to the absence of epidermis.[19]

Another mechanism is; the crawling of individual cells over each other at the tip of the regenerating epidermis. At this site, the supra basal keratinocytes had a migratory phenotype and expressed laminin 5due to the altered keratinocyte polarity at the wound margin which help migration through supporting keratinocyte motility and the establishment of hemi-desmosomes.[19]

The early reepithelization detected in the current study on day 14 in groups II and III in comparison to group I could be attributed to one of the features of the ADM prepared and applied in these groups which is the retention of the intact basement membrane.

Recently, Fisher & Rittié[20] reported that basement membrane at the dermo-epidermal junction determines the polarity of the epidermis, thereby controlling cell organization and differentiation and that its repair during wound healing is important for restoration of skin functional properties after wounding.

Moreover, the importance of basement membrane integrity in the normal process of wound healing has been reported by many other studies, which demonstrated that lake of intact basement membrane resulted in the formation of fragile skin and blistering problems.[20–22] In this study, collagen in the dermis was disorganized and arranged into granulation tissue in group I on day 14. While, on day 28, thin, disorganized collagen fibers were detected. In contrast, in groups II and III the application of a biological matrix scaffold (ADM) onto the wound site favored the appearance of well- organized collagen bundles comparable to normal skin.

Furthermore, statistical analysis confirmed the significant increase in area percentage of collagen in wounds treated with seeded ADM (group III) in comparison to the other 2 groups. Likewise, wounds treated with unseeded ADM (group II) showed a significant increase in area percentage of collagen in comparison to wounds left for spontaneous healing (group I). These results might be explained on the basis that, in the absence of an established dermal matrix, fibroblasts initially synthesize an immature matrix, which is subsequently remodeled to form scar. On the other hand, fibroblasts that repopulate the acellular matrix maintain their capacity to produce a more mature collagen.[13]

Additionally, the preservation of ECM in ADM influence cell mitogenesis and chemotaxis, direct cell differentiation, and induce constructive host tissue remodeling responses, and the presence of residual cellular material attenuates or fully disproves the constructive tissue remodeling advantages of biologic scaffold materials *in vivo* .[12] In the present study, applying MSCs seeded ADM onto the wound site, provided the best results in comparison to the other groups as regarding early reepithelization, collagen organization into thick bundles, and resolution of inflammation. Furthermore, skin appendages were detected in the dermis and were fully developed. These results were further confirmed by statistical analysis which illustrated that treatment of wounds by seeded ADM (group III) resulted in a significant increase in wound healing rate over the last 2 weeks, percent reduction in wound area in comparison to treatment with unseeded ADM (group II) and spontaneous recovery (group I). These findings were approved by other studies which demonstrated that MSCs transplantation in the wounded skin can successfully differentiate into epidermal keratinocytes, sebaceous glands and follicular epithelial cells.[23,24] Moreover, delivery of BM-MSCs in collagen gel scaffolds to full thickness skin wounds of rats resulted in significant early reduction in wound size in rats treated with MSC-collagen scaffold compared to collagen alone.[25]

Although MSCs differentiation contributes to regeneration of damaged or absent tissues, their paracrine signaling by releasing biologically active molecules is likely the primary mechanism for the beneficial effects of MSCs on wounds, through affecting cell migration, proliferation, and survival of the surrounding cells.[16] Moreover, analyses of MSC-conditioned medium indicated that, MSCs secrete many known mediators of tissue repair including growth factors, cytokines, chemokines, keratinocyte growth factor, and TGF-β and that many cell types, including epithelial cells, endothelial cells, keratinocytes, and fibroblasts, are responsive to these paracrine signaling factors.[16,26] Statistical analysis of vascular density in the current study revealed that applying seeded ADM onto the wound resulted in early (day 14) significant increase vascular density in comparison to the unseeded ADM or spontaneous healing. On the contrary, spontaneous healing resulted in late (day 28) marked significant increase in vascular density in comparison to the treated group.

We assumed that applying ADM, in particular seeded matrix, resulted in rapid progression of wound healing from the proliferative phase in which neovascularization increase to the remolding phase in which neovascularization is minimal. This assumption was supported statistically by the significant increase of wound healing rate in the treated groups in comparison to spontaneous healing. In this view, Sorg et al.[27] reported that, angiogenesis in wound healing can be divided into two main phases. Pro-angiogenic phase in which excessive neo-formation of blood vessels occurs to restore blood flow and thus nutritive perfusion as quickly as possible. This is followed by an anti-angiogenic phase in which the initially established vascular network undergoes a maturing process, which, however, is accompanied by a significant reduction in the number of vessels. Moreover, it was reported that, treating wound with MSC-collagen scaffold resulted in early wound closure in association with increased angiogenesis due to significant expression of vascular endothelial growth factor (VEGF) and more intense early expression of matrix metalloproteinase -9 (MMP-9) compared to collagen treatment without MSCs, indicating a possible mechanism of MSC's effects on early wound healing.[28] In conclusion, application of ADM onto skin wound greatly improves wound healing on the gross and microscopic structure level. Furthermore, MSCs seeded ADM, provides much better results in terms of duration and restoration of skin structures.

Acknowledgments

None.

Conflicts of interest

Authors declare that there is no conflicts of interest.

References

1. Herndon DN, Barrow RE, Rutan RL, et al. Comparison of conservative versus early excision. Therapies in severely burned patients. *Ann Surg*.1989;209(5):547–552.
2. Ruszczak Z. Effect of collagen matrices on dermal wound healing. *Adv Drug Delivery Rev*. 2003;55(12):1595–1611.
3. Shin H, Jo S, Mikos AG. Biomimetic materials for tissue engineering. *Biomaterials*. 2003;24(24): 4353–4364.
4. Del BakhshayeshaA R, Annabic N, Khalilovf R, et al. Recent advances on biomedical applications of scaffolds in wound healing and dermal tissue engineering. *Artificial Cells, Nanomedicine, and Biotechnology*. 2017;46(6):1–15.
5. Walter RJ, Matsudab T, Reyes HM, et al. Characterization of acellular dermal matrices (ADMs) prepared by two different methods. *Burns*. 1989;24(2):104–113.
6. Lee DE, Ayoub N, Agrawal DK. Mesenchymal stem cells and cutaneous wound healing: novel methods to increase cell delivery and therapeutic efficacy. *Stem Cell Research and Therapy*. 2016;7:37–44.

7. Lennon DP, Caplan AI. Isolation of rat marrow–derived mesenchymal stem cells. *Exp Hematol*. 2006;34(11):1606–1607.
8. Shao–Fang Z, Hong–Tian Z, Zhi–Nian Z, et al. PKH26 as a fluorescent label for live human umbilical mesenchymal stem cells. *In Vitro Cell Dev Biol Anim*. 2011;47(8):516–520.
9. Zhang X, Deng Z, Wang H, et al. Expansion and delivery of human fibroblasts on micronized acellular dermal matrix for skin regeneration. *Biomaterials*. 2009;30(14):2666–2674.
10. Arnold TE, Stanley JC, Fellows EP, et al. Prospective, Multicenter study of managing lower extremity venous ulcers. *Ann Vasc Surg*. 1991;8(4):356–362.
11. Cukjati D, Rebersek S, Miklavcic D. A reliable method of determining wound healing rate. *Medical & Biological Engineering & Computing*. 2001;39(2):263.
12. Crapo PM, Gilbert TW, Badylak SF. An overview of tissue and whole organ decellularization processes. *Biomaterials*. 2011;32(12):3233–3243.
13. Wainwright DJ. Use of an acellular allograft dermal matrix (AlloDerm) in the management of full–thickness burns. *Burns*. 1995;21(4);243–248.
14. Ge L, Zheng S, Wei H. Comparison of histological structure and biocompatibility between human acellular dermal matrix (ADM) and porcine ADM. *Burns*. 2009;35(1):46–50.
15. Badylak SF. The extracellular matrix as a biologic scaffold material. *Biomaterials*. 2007;28(25):3587–3593.
16. Maxson S, Lopez EA, Yoo D, et al. Concise Review: Role of Mesenchymal Stem Cells in Wound Repair. *Stem Cells Translational Medicine*. 2012;1(2):142–149.
17. Feng X, Shen R, Tan J, et al. The study of inhibiting systematic inflammatory response syndrome by applying xenogenic (porcine) acellular dermal matrix on second-degree burns. *Burns*. 2007;33(4):477–479.
18. Mei SH, Haitsma JJ, Dos Santos CC, et al. Mesenchymal stem cells reduce inflammation while enhancing bacterial clearance and improving survival in sepsis. *Am J Respir Crit Care Med*. 2010;182(8):1047–1057.
19. Laplante A, Germain L, Auger FA, et al. Mechanisms of wound re-epithelialization: hints from a tissue–engineered reconstructed skin to long–standing questions. *FASEB*. 2001;15(13):2377–2389.
20. Fisher G, Rittié L. Restoration of the basement membrane after wounding: a hallmark of young human skin altered with aging. *J Cell Commun Signal*. 2018;12(1):401–411.
21. Bruckner–Tudermanab L, Has C. Disorders of the cutaneous basement membrane zone–The paradigm of epidermolysis bullosa. *Matrix Biology*. 2014;33:29–34.
22. Sebastian M, Jan E, Dieter M. Blistering and Skin Fragility Due to Imatinib Therapy: Loss of Laminin and Collagen IV as a Possible Cause of Cutaneous Basement Membrane Instability. *Am J Dermatol*. 2018;40(5):371–374.
23. Nakagawa H, Akita S, Fukui M, et al. Human mesenchymal stem cells successfully improve skin–substitute wound healing. *Br J Dermatol*. 2005;153(1):29–36.
24. Dash BC, Xu Z, Lin L, et al. Stem Cells and Engineered Scaffolds for Regenerative Wound Healing. *Bioengineering*. 2018;5(1):23–42.
25. Kim CH, Lee JH, Won JH, et al. Mesenchymal stem cells improve wound healing in vivo via early activation of matrix metalloproteinase–9 and vascular endothelial growth factor. *J Korean Med Sci*. 2011;26(6):726–733.
26. Gnecchi M, Zhang Z, Ni A, Dzau VJ. Paracrine mechanisms in adult stem cell signaling and therapy. *Circ Res*. 2008;103(11):1204 –1219.
27. Sorg H, Tilkorn DJ, Mirastschijski U, et al. Panta Rhei: Neovascularization, angiogenesis and nutritive perfusion in wound healing. *Eur Surg Res*. 2018;59:232–241.
28. Oloughlin A, Kulkarni M, Creane M, et al. Topical administration of allogeneic mesenchymal stromal cells seeded in a collagen scaffold augments wound healing and increases angiogenesis in the diabetic rabbit ulcer. *Diabetes*. 2013;62(7):2588–2594.